

Technical Paper 3683



X-38 Vehicle 131 Flutter Assessment

James P. Smith

May 1997

1N-16
030608

1000 2000 3000

1000 2000 3000 4000 5000 6000 7000 8000 9000 10000

1000 2000 3000 4000 5000 6000 7000 8000 9000 10000

Technical Paper 3683

X-38 Vehicle 131 Flutter Assessment

James P. Smith

Lyndon B. Johnson Space Center

May 1997

National Aeronautics
and Space Administration

Lyndon B Johnson Space Center
Houston, Texas 77058-4406

This publication is available from the Center for AeroSpace Information, 800 Elkridge Landing Road,
Linthicum Heights, MD 21090-2934 (301) 621-0390

Contents

Acronyms	iv
Abstract	1
Introduction	1
Vehicle Fin Properties	1
Three-Dimensional NASTRAN Dynamic Model	2
Three-Dimensional NASTRAN Modal Analysis	2
Experimental Modes of the Fin	5
Test Modes of the Free Rudder Fin	5
Test Modes of the Shimmed Rudder Fin	8
Assumed Fin Modes for Flutter Analysis	16
NASTRAN Fin Flutter Aerodynamic Model	16
NASTRAN Flutter Analysis Results	16
Prediction of Classical State Divergence of the Fin	20
Aileron Buzz Prediction of the Fin	22
References	23

Tables

1	Density Ratios Used in NASTRAN Flutter Analysis	20
2	Aileron Buzz Dynamic Pressure and Mach Number	23

Figures

1	X-38 Vehicle 131 flight envelope	1
2	X-38 Vehicle 131 fin geometry	2
3	Finite element mesh of the three-dimensional fin region	3
4	Undeformed configuration of the fin region	3
5	First analytical mode (27.011 Hz) of the fixed rudder fin	4
6	Second analytical mode (38.518 Hz) of the fixed rudder fin	4
7	Third analytical mode (61.108 Hz) of the fixed rudder fin	5
8	First analytical mode (24.734 Hz) of the free rudder fin	6
9	Second analytical mode (36.073 Hz) of the free rudder fin	6

Contents

(concluded)

10	Third analytical mode (41.311 Hz) of the free rudder fin.....	7
11	Fourth analytical mode (62.570 Hz) of the free rudder fin.....	7
12	First vehicle mode (22.8447 Hz) of the free rudder configuration.....	8
13	Second vehicle mode (24.0835 Hz) of the free rudder configuration.....	9
14	Third vehicle mode (36.771 Hz) of the free rudder configuration.....	9
15	Fourth vehicle mode (43.1072 Hz) of the free rudder configuration.....	10
16	Fifth vehicle mode (46.8438 Hz) of the free rudder configuration.....	10
17	Sixth vehicle mode (51.9867 Hz) of the free rudder configuration.....	11
18	Seventh vehicle mode (56.8324 Hz) of the free rudder configuration.....	11
19	Eighth vehicle mode (67.1932 Hz) of the free rudder configuration.....	12
20	First vehicle mode (24.1905 Hz) of the fixed rudder configuration.....	12
21	Second vehicle mode (25.6099 Hz) of the fixed rudder configuration.....	13
22	Third vehicle mode (32.9298 Hz) of the fixed rudder configuration.....	13
23	Fourth vehicle mode (42.7590 Hz) of the fixed rudder configuration.....	14
24	Fifth vehicle mode (46.8017 Hz) of the fixed rudder configuration.....	14
25	Sixth vehicle mode (56.3088 Hz) of the fixed rudder configuration.....	15
26	Seventh vehicle mode (65.3449 Hz) of the fixed rudder configuration.....	15
27	Eighth vehicle mode (71.4987 Hz) of the fixed rudder configuration.....	16
28	Finite element mesh of the planar fin model.....	17
29	First planar model mode (22.8447 Hz) of fin.....	17
30	Second planar model mode (36.7710 Hz) of fin.....	18
31	Third planar model mode (43.1072 Hz) of fin.....	18
32	Fourth planar model mode (67.1932 Hz) of fin.....	19
33	Aerodynamic grid for the fin model.....	19
34	Damping and frequency curves for sea level.....	20
35	Damping and frequency curves for 10,000 ft.....	21
36	Damping and frequency curves for 20,000 ft.....	21
37	Damping and frequency curves for 30,000 ft.....	21
38	Damping and frequency curves for 40,000 ft.....	22

Abstract

Contained herein are the findings from the X-38 vehicle 131 flutter prediction program at the NASA/Johnson Space Center. The results presented show the 131 vehicle to be flutter free in the maximum flight profile of $q = 500$ psf.

Introduction

The X-38 is a space vehicle being developed at the NASA Johnson Space Center (JSC) for the primary purpose of transporting crew from the International Space Station during an emergency situation. Other options for the vehicle have included the transport of crew from Earth to International Space Station with the vehicle serving as a payload on a traditional launch system.

One of the test articles used in the development of the X-38 is the Vehicle 131 (V131), a fiberglass and metallic structure based on the mold lines of the X-24 shape and built by Scaled Composites, Inc., of Mojave, California. Equipped with avionics and a landing system similar to the X-38 baseline, the V131 will be drop-tested from a B-52 aircraft at the NASA Dryden Space Flight Center.

The operational environment of the V131 is such that the maximum dynamic pressure shall not be above 500 psf. Figure 1 shows the flight envelopes of the B-52 and V131. For flutter, the speeds at which flutter occurs shall have a 15% safety factor applied, as specified by [3]. It will be shown, however, that the predictions for flutter are outside the flight envelope of the V131.

The flutter analysis involved both analytical results and experimental ground modal test results. The flutter analysis tool used analytical modes shapes correlated to the experimental modes. We ran several cases, which included mixed flight Mach numbers, velocities, and density ratios. In this report, we report the worst-case analysis.

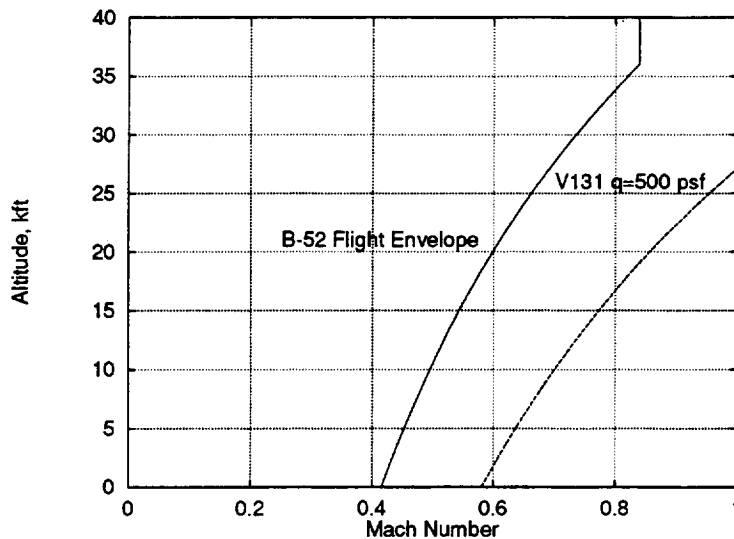


Figure 1. X-38 Vehicle 131 flight envelope.

Vehicle Fin Properties

Figure 2 shows the approximate dimensions of the V131 fin. The fin is actually three-dimensional in construction rather than planar. The aft portion of the fin has an outward bend, providing a different

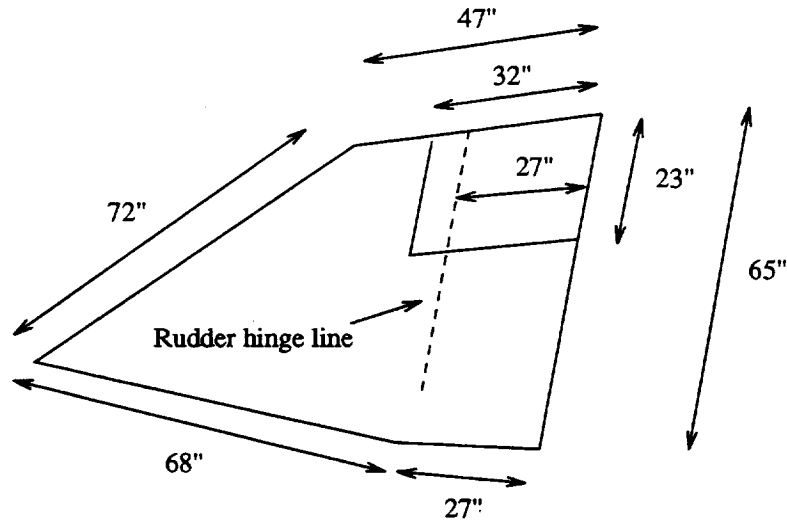


Figure 2. X-38 Vehicle 131 fin geometry.

angle of attack from the forward portion of the fin.

A knife edge test of the rudder found a rudder mass of $.04335 \text{ lb-sec}^2/\text{in}$, or 16.75 pounds under 1g. The center of mass of the rudder lies approximately 8.33 inches behind the rudder hinge line. The mass moment of inertia about the hinge line is 7.6 lb-in-sec^2 (20.40 lb-ft^2).

The fin is comprised mostly of fiberglass and balsa core material. The inboard and outboard surfaces of the fin have face sheets with thickness .06 inches separated by a balsa core of .5 inches. The mass density of the composite face sheet is $.0001554 \text{ lb-sec}^2/\text{in}^4$, and the mass density of the balsa core is $.0000178 \text{ lb-sec}^2/\text{in}^4$.

Three-Dimensional NASTRAN Dynamic Model

To correlate the experimental modal results, we generated a three-dimensional finite element math model. The model, shown in Figure 3, contains only information on the aft portion of the vehicle. Scaled Composites, Inc. furnished the detailed model of the fin without the attached rudder. Later, we added the rudder and vehicle acreage and the body structure to provide a better representation of the overall fin stiffness. The initial model used clamped boundary conditions at the edge of the fin which provided inaccurate fin vibration modes.

Three-Dimensional NASTRAN Modal Analysis

We executed a NASTRAN modal analysis of the three-dimensional model to compare the analytical model to the physical model and to provide mode shapes for a subsequent flutter analysis. Two configurations of the model shown in Figure 3 were run. In the first configuration, the rudder was rigidly attached to the fin to prevent rudder rotation. Figure 4 shows the undeformed model in the region of the fin. The mode of Figure 5 with a frequency of $f = 27.011 \text{ Hz}$ represents the first analytical fin bending mode. At $f = 38.518 \text{ Hz}$, the outboard panel of the fin vibrates, causing some fin tip motion, as seen in Figure 6. Finally, Figure 7 shows a torsion mode at $f = 61.108 \text{ Hz}$.

In the second configuration, the rudder freely rotates, and elements representing the rudder torque tube stiffness, the actuator system stiffness, and local structural attach stiffness provide stiffness. The

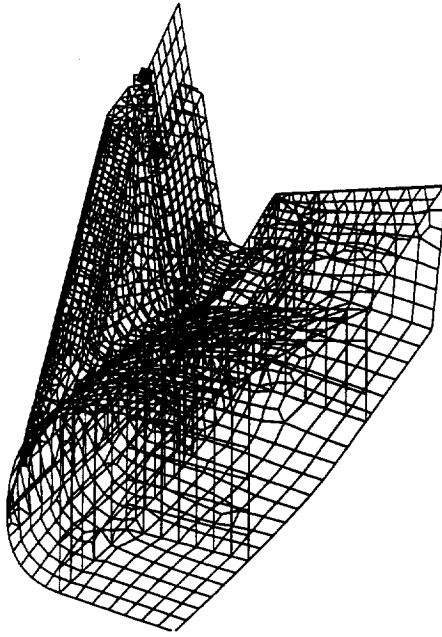


Figure 3. Finite element mesh of the three-dimensional fin region.

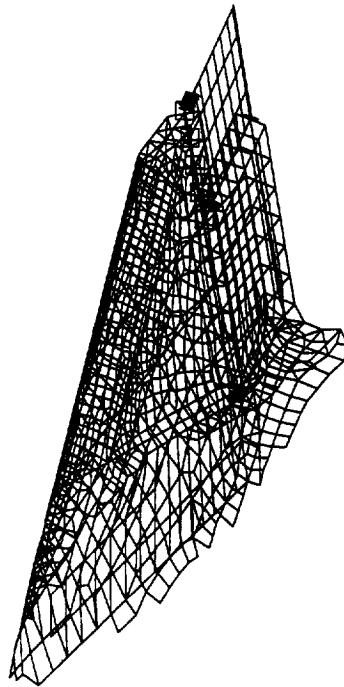


Figure 4. Undeformed configuration of the fin region.

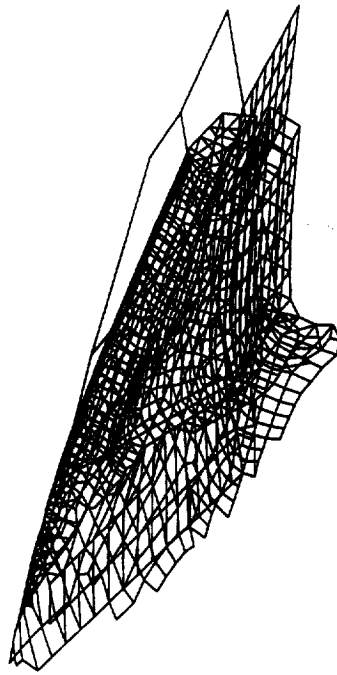


Figure 5. First analytical mode (27.011 Hz) of the fixed rudder fin.

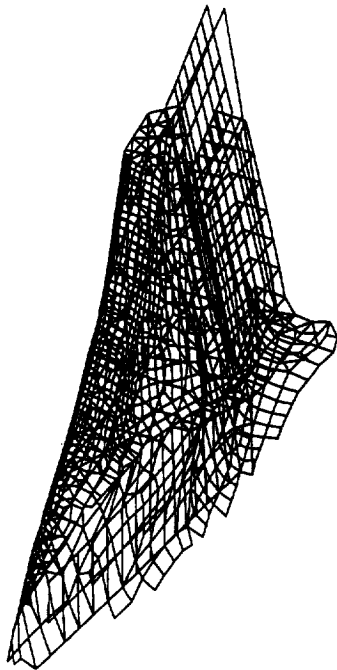


Figure 6. Second analytical mode (38.518 Hz) of the fixed rudder fin.

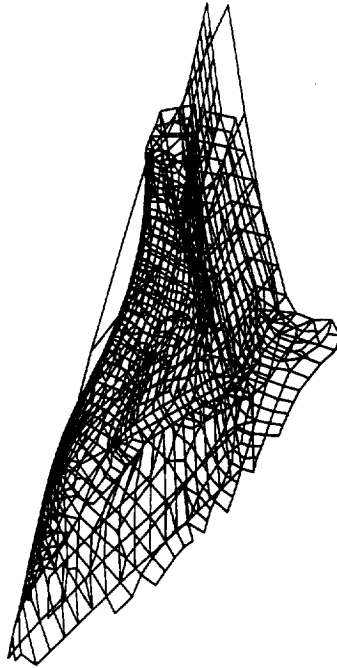


Figure 7. Third analytical mode (61.108 Hz) of the fixed rudder fin.

mode of Figure 8 with a frequency of $f = 24.734$ Hz represents the first analytical fin bending mode. At $f = 36.073$ Hz, the outboard panel of the fin vibrates, causing some fin tip motion, as seen in Figure 9. Figure 10 shows similar mode at a frequency of $f = 41.311$ Hz. Finally, Figure 11 shows a torsion mode at $f = 62.570$ Hz.

Experimental Modes of the Fin

We conducted a modal test of the V131 to characterize the dynamic characteristics of the fins, and we suspended the vehicle by two cables at a forward and aft point on the top of the structure. A total of 95 accelerometer channels described the modes of vibration, with the majority of the channels devoted to the fin regions. We placed a shaker on the main structure of the port fin at the aft trailing edge just below the rudder. The shaker provided a random signal at 12.5 N, 25 N, and 50 N levels. The vehicle was tested in two configurations. In the first case, a soft spring connected the two rudders to reduce the amount of freeplay in the rudder system, which can cause nonlinearities in the test results. The measured freeplay in the rudder was no more than $.13^\circ$, which is within the required allowable rudder freeplay [3]. In the second configuration, shims placed between the rudder and the fin prevented independent motion of the rudder. This fixed rudder configuration is representative of a highly stiff rudder system circuit stiffness.

Test Modes of the Free Rudder Fin

Figure 12 to Figure 19 show the first eight modes corresponding to the configuration with the rudders tied together. In the figures, the solid line denotes the undeformed configuration, and the dashed line

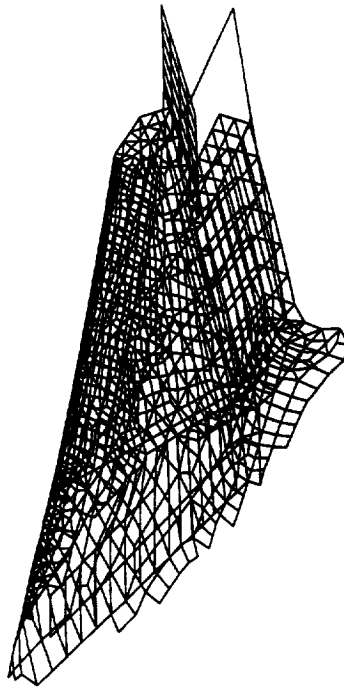


Figure 8. First analytical mode (24.734 Hz) of the free rudder fin.

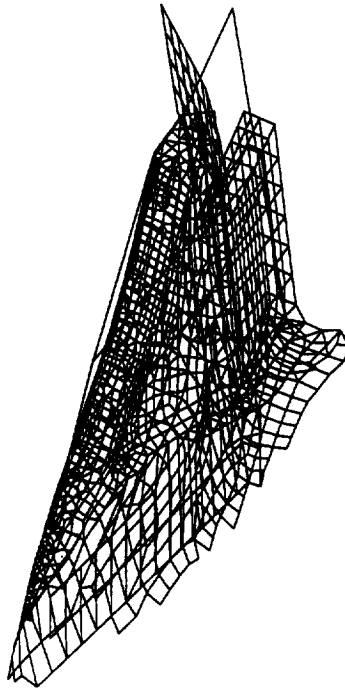


Figure 9. Second analytical mode (36.073 Hz) of the free rudder fin.

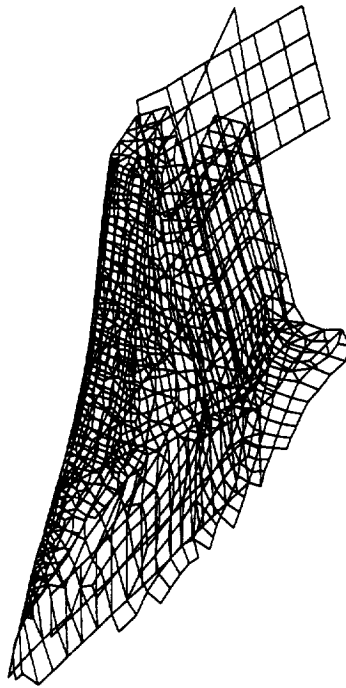


Figure 10. Third analytical mode (41.311 Hz) of the free rudder fin.

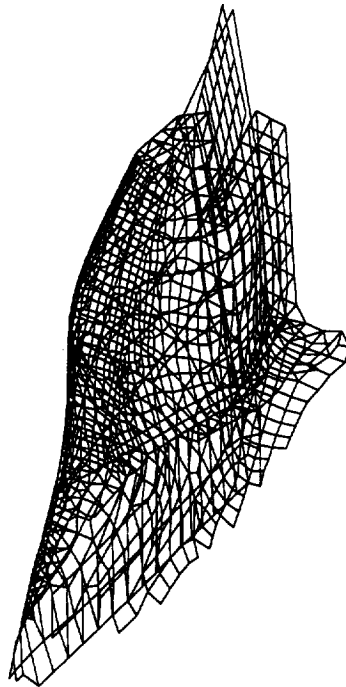


Figure 11. Fourth analytical mode (62.570 Hz) of the free rudder fin.

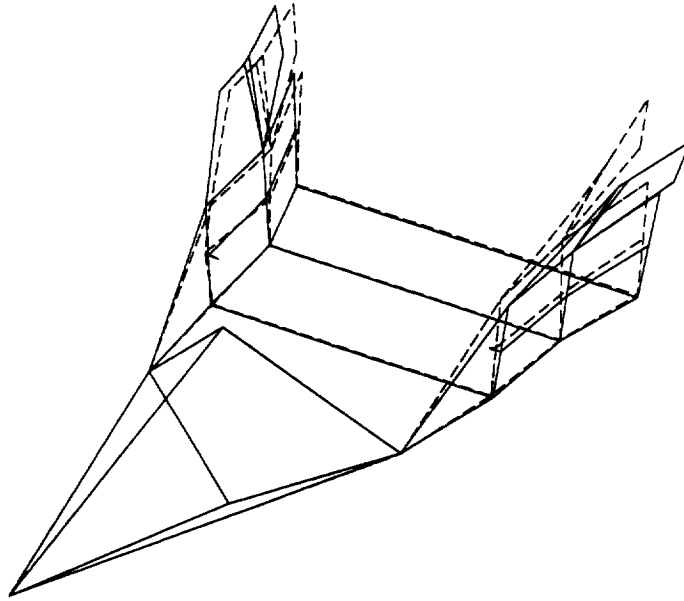


Figure 12. **First vehicle mode (22.8447 Hz) of the free rudder configuration.**

represents the deformed shape. The mode of Figure 12 is a symmetric fin and rudder bending mode with a frequency of 22.84 Hz. The second mode, shown in Figure 13, is an antisymmetric fin and rudder bending mode with a frequency of 24.08 Hz. The mode of Figure 14 with a frequency of 36.77 Hz is primarily a rudder mode. Figure 15 shows a symmetric mode consisting of panel vibration on the outboard panels of the fins and rudder rotation at 43.11 Hz. Figure 16 shows a similar mode at 46.84 Hz, where the mode appears to be superimposed on an overall vehicle bending mode. Figure 17 shows a higher rudder mode at 52.00 Hz. This mode appears to be the same type of mode as the one of Figure 14, but on the opposite fin, suggesting that the linkage system on the starboard rudder is stiffer than the port system. Figure 18 shows a panel mode couple with a twisting mode of the starboard rudder at 56.83 Hz. Finally, Figure 19 shows a symmetric torsion mode at 67.19 Hz.

Test Modes of the Shimmed Rudder Fin

Figure 20 to Figure 27 show the first eight modes corresponding to the configuration with the rudders shimmed. In the figures, the solid line denotes the undeformed configuration, and the dashed line represents the deformed shape. The mode of Figure 20 is a symmetric fin bending mode with a frequency of 24.19 Hz. The second mode, shown in Figure 21, is an antisymmetric fin bending mode with a frequency of 25.61 Hz. The mode of Figure 22 with a frequency of 32.93 Hz is a panel mode consisting of panel vibration of the outboard panels of the fins. Figure 23 shows a mode consisting of symmetric panel vibration on the outboard panels of the fins and antisymmetric bending at 42.76 Hz. Figure 24 shows a panel and vehicle bending mode at 46.80 Hz. A symmetric panel and bending mode at 56.31 Hz is seen in Figure 25. This mode is similar to the mode of Figure 22. Figure 26 shows a torsion mode of the starboard fin and some torsion in the port fin at 65.34 Hz. Finally, Figure 27 shows an antisymmetric torsion mode at 71.50 Hz.

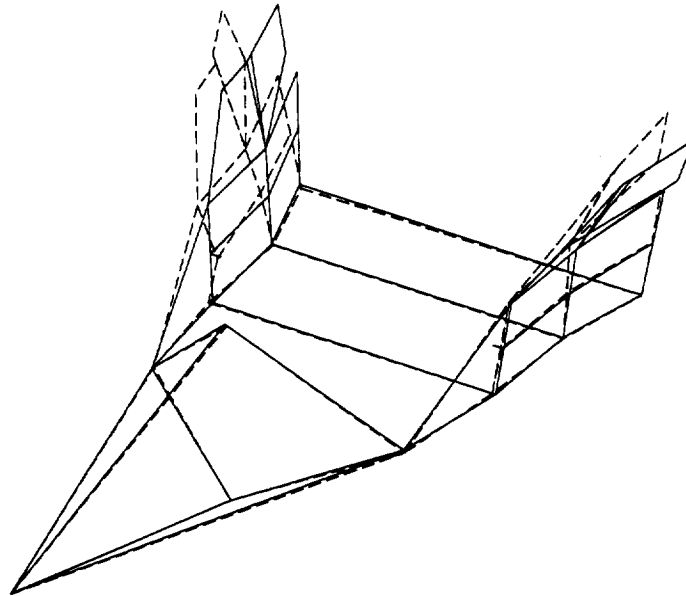


Figure 13. **Second vehicle mode (24.0835 Hz) of the free rudder configuration.**

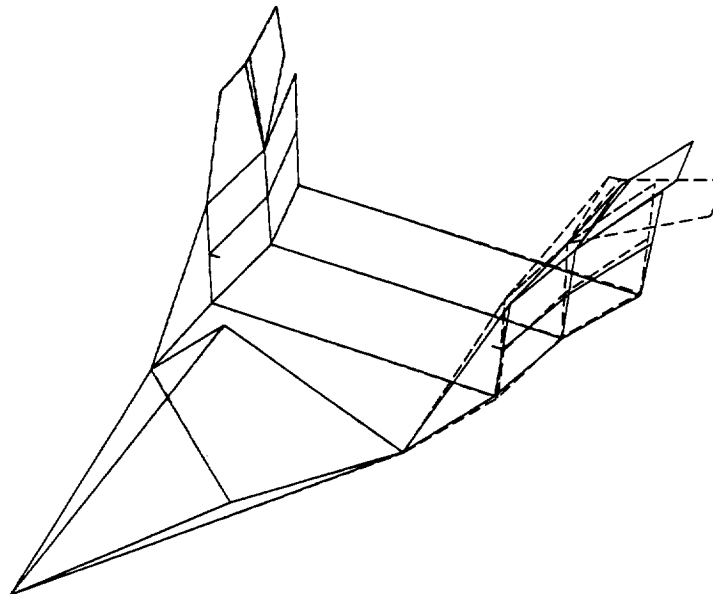


Figure 14. **Third vehicle mode (36.771 Hz) of the free rudder configuration.**

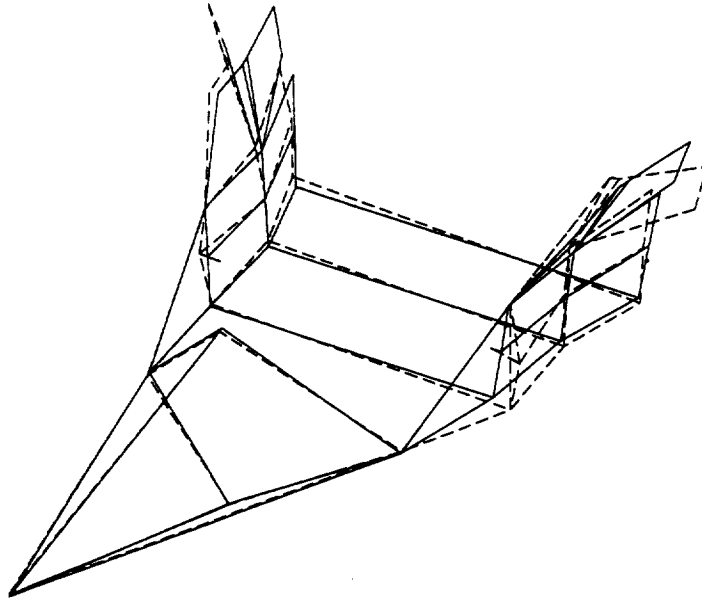


Figure 15. **Fourth vehicle mode (43.1072 Hz) of the free rudder configuration.**

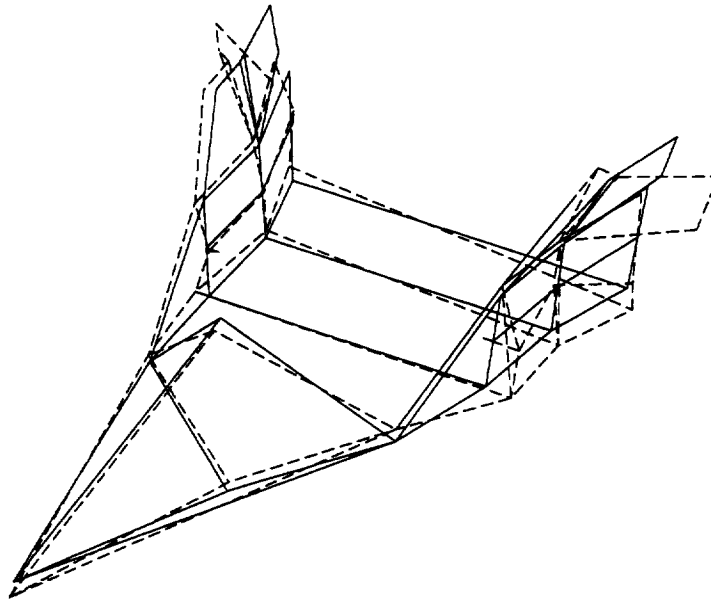


Figure 16. **Fifth vehicle mode (46.8438 Hz) of the free rudder configuration.**

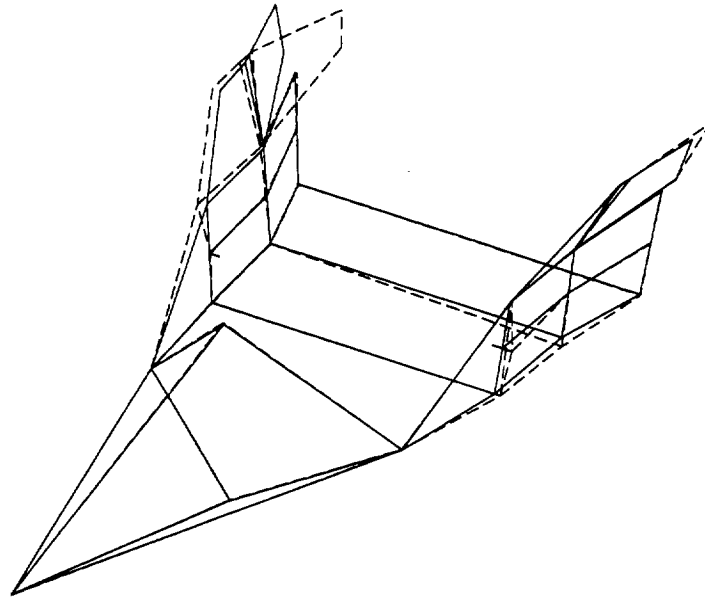


Figure 17. **Sixth vehicle mode (51.9867 Hz) of the free rudder configuration.**

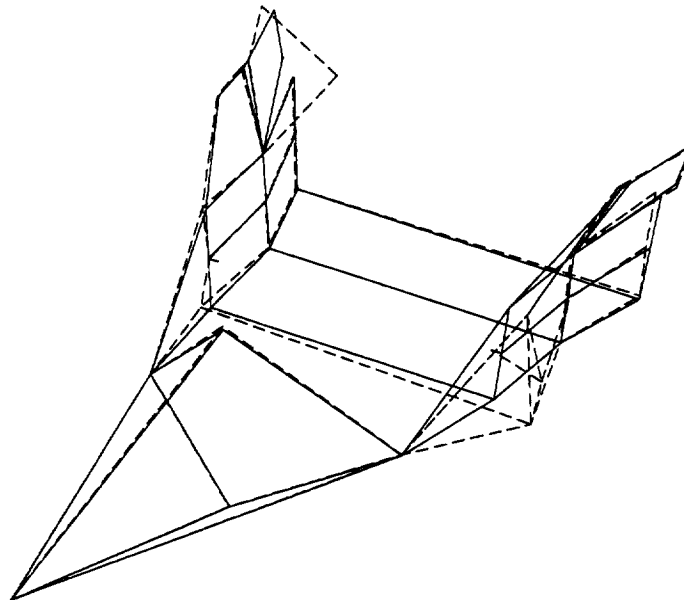


Figure 18. **Seventh vehicle mode (56.8324 Hz) of the free rudder configuration.**

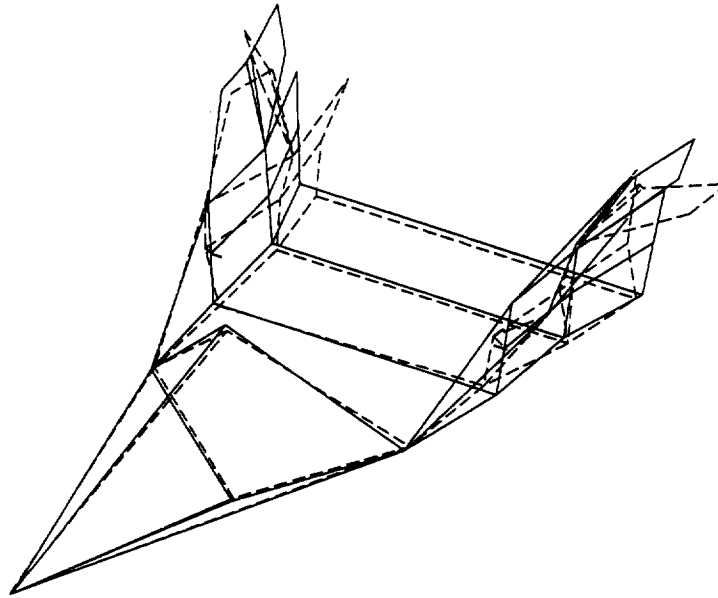


Figure 19. **Eighth vehicle mode (67.1932 Hz) of the free rudder configuration.**

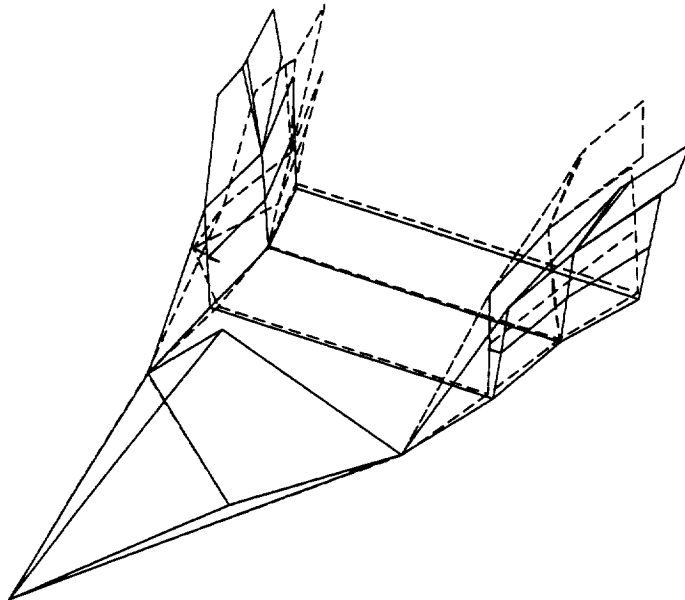


Figure 20. **First vehicle mode (24.1905 Hz) of the fixed rudder configuration.**

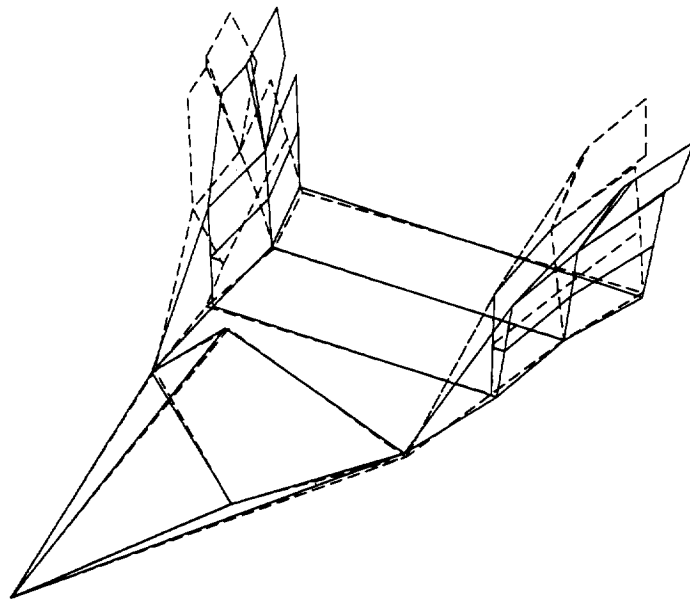


Figure 21. **Second vehicle mode (25.6099 Hz) of the fixed rudder configuration.**

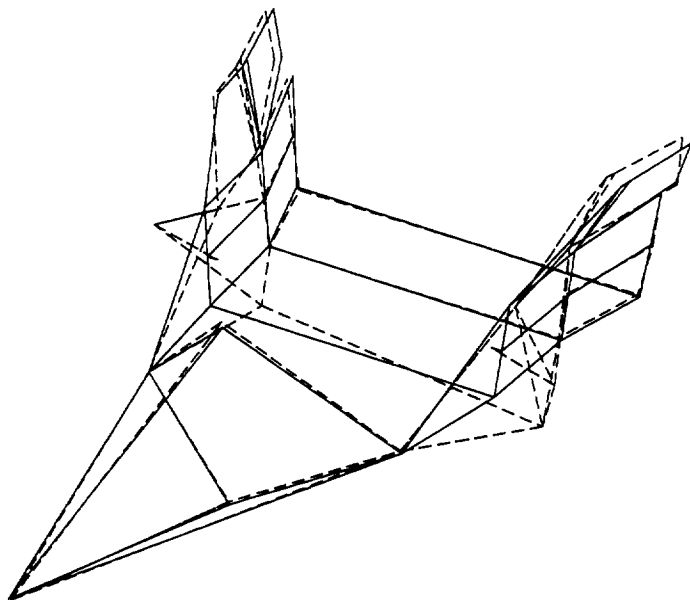


Figure 22. **Third vehicle mode (32.9298 Hz) of the fixed rudder configuration.**

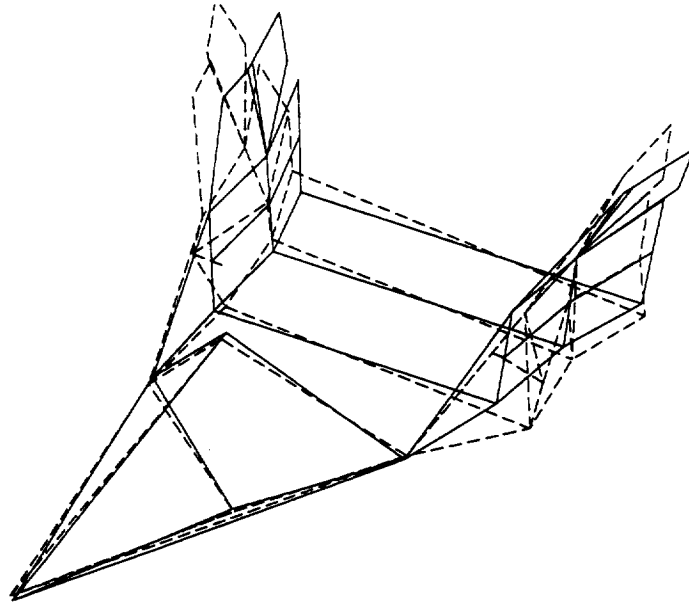


Figure 23. **Fourth vehicle mode (42.7590 Hz) of the fixed rudder configuration.**

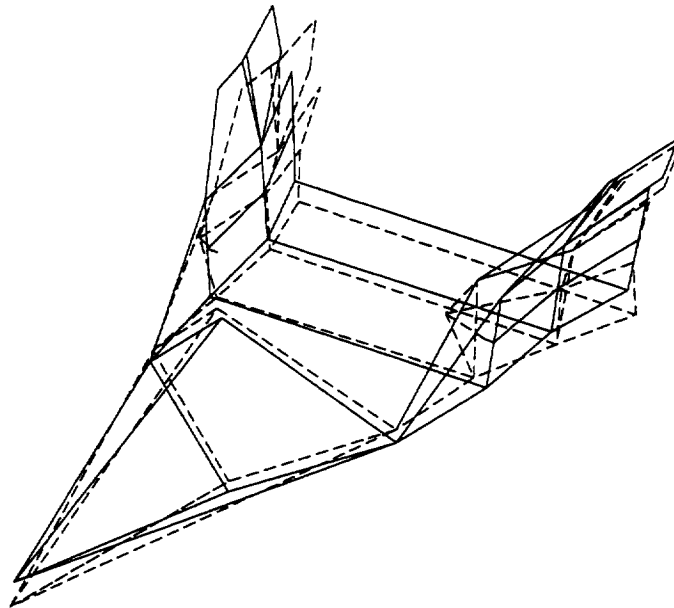


Figure 24. **Fifth vehicle mode (46.8017 Hz) of the fixed rudder configuration.**

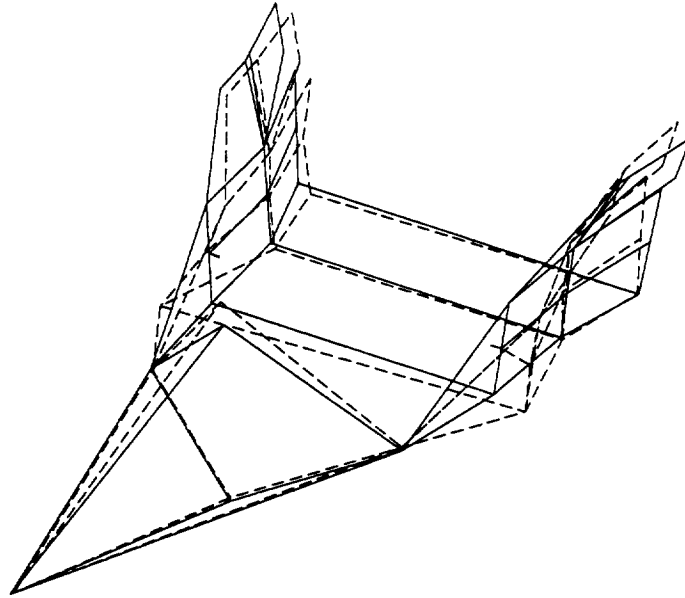


Figure 25. Sixth vehicle mode (56.3088 Hz) of the fixed rudder configuration.

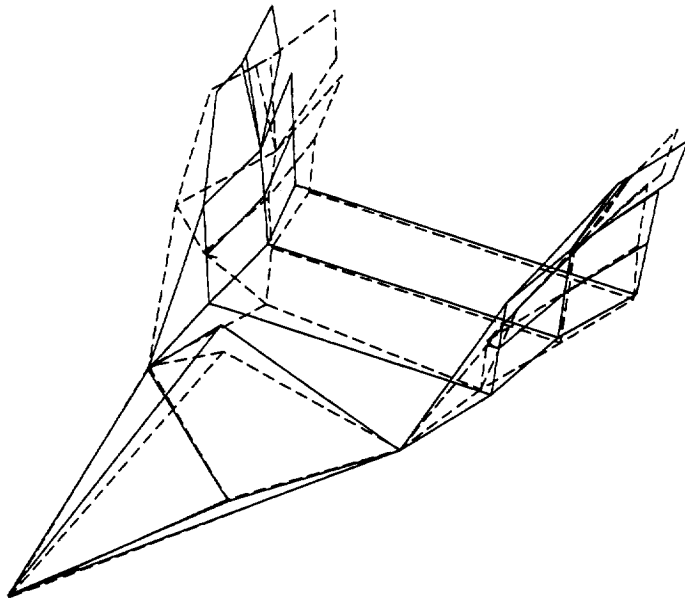


Figure 26. Seventh vehicle mode (65.3449 Hz) of the fixed rudder configuration.

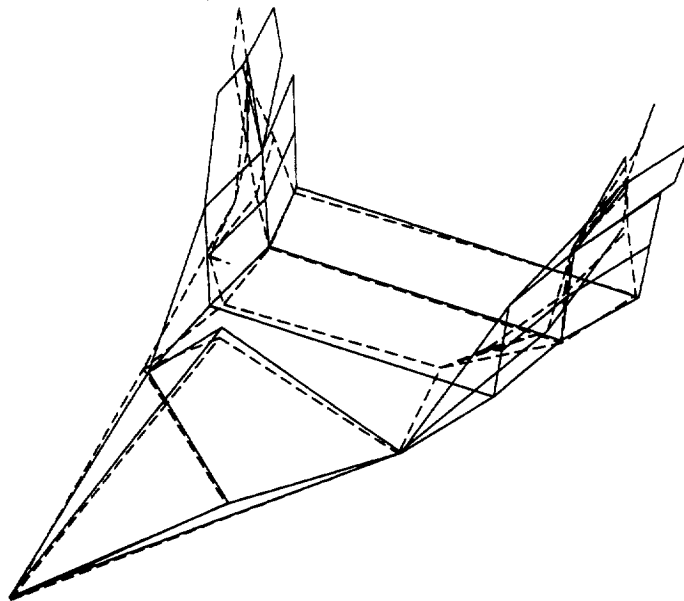


Figure 27. Eighth vehicle mode (71.4987 Hz) of the fixed rudder configuration.

Assumed Fin Modes for Flutter Analysis

We wrote a FORTRAN computer program to map the displacements of the three-dimensional model onto the planar fin model shown in Figure 28. Thus, the assumed fin modes are averages of the deflections on the inboard and outboard surfaces of the fin. The modes are based on the analytical modes from the NASTRAN modal analysis and the frequencies are based on the experimental test results from the V131 modal test. Figure 29 to Figure 32 show the modes of vibration for the planar model corresponding to the modes of Figure 8 to Figure 11.

NASTRAN Fin Flutter Aerodynamic Model

Figure 33 shows the aerodynamic model used for the flutter calculations in NASTRAN. We used a total of six aerodynamic panel elements with each panel having ten chordwise boxes. We invoked Doublet-Lattice theory aerodynamics and the PK-method of flutter analysis. We performed the flutter analysis at the densities shown in Table 1, which correspond to altitudes ranging from sea level to 40,000 ft. The velocities ranged from 1000 in/sec to 15000 in/sec. The structure had minimal structural damping of .05%. The fin has a reference chord of 62.86 inches, and the rudder has a chord length of 32 inches. Since one-half of the model was used, model symmetry is assumed in the geometry and deformations.

NASTRAN Flutter Analysis Results

Figure 34 to Figure 38 show the results of the flutter analysis in the form of damping and frequency curves. The only case where positive damping is encountered is the sea-level case, where instabilities occur at 1200 ft/sec, which corresponds to a dynamic pressure of $q = 1712$ psf and a Mach number greater than 1.0. If we apply a 1.15 factor of safety to the velocity, then $q = 1295$ psf, which is outside

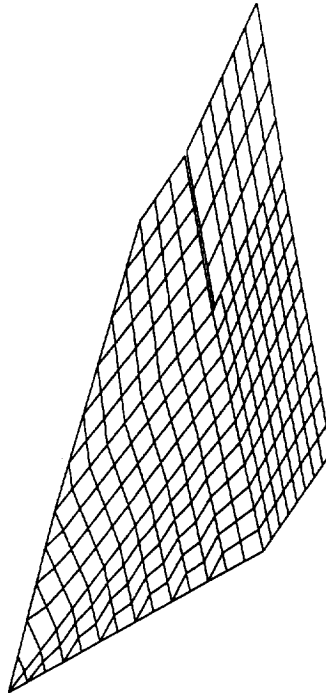


Figure 28. **Finite element mesh of the planar fin model.**

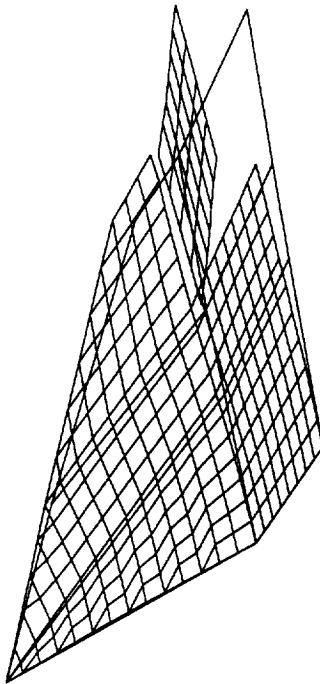


Figure 29. **First planar model mode (22.8447 Hz) of fin.**

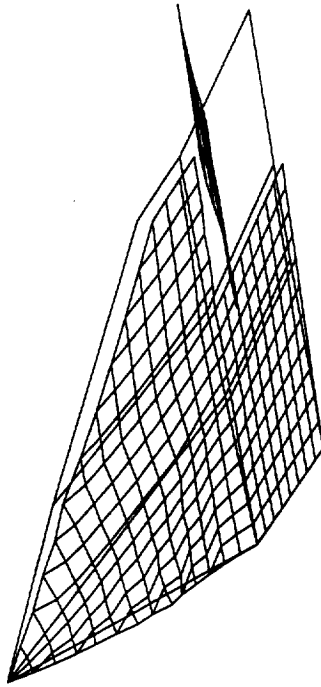


Figure 30. Second planar model mode (36.7710 Hz) of fin.

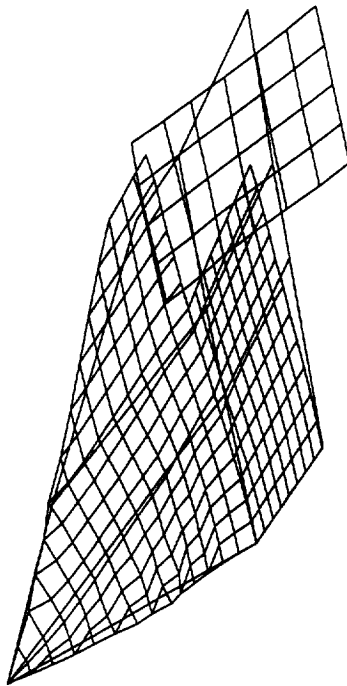


Figure 31. Third planar model mode (43.1072 Hz) of fin.

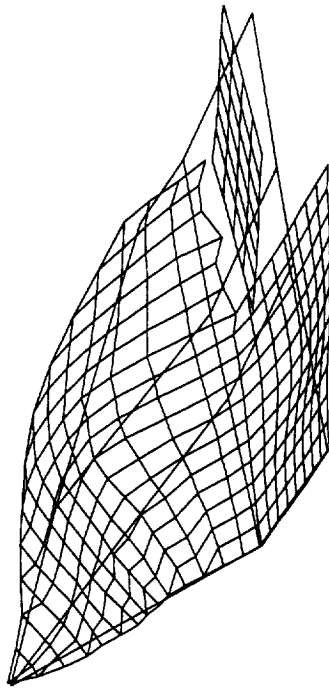


Figure 32. Fourth planar model mode (67.1932 Hz) of fin.

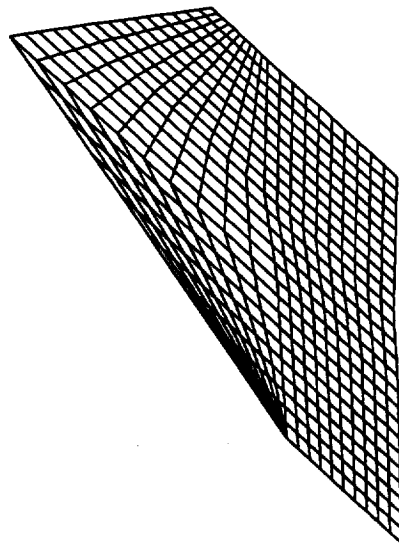


Figure 33. Aerodynamic grid for the fin model.

Table 1. Density Ratios Used in NASTRAN Flutter Analysis

Altitude (kft)	ρ (lb-sec ² /in ⁴)
0	1.1472E-7
10	.847E-7
20	.611E-7
30	.4291E-7
40	.2823E-7

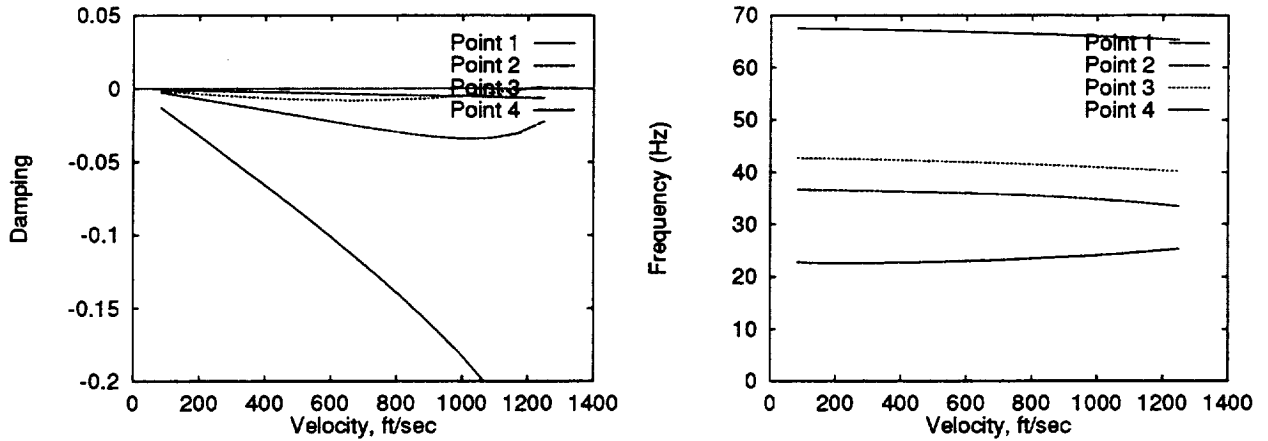


Figure 34. Damping and frequency curves for sea level.

the baselined flight envelope.

We performed additional finite element analysis to assess the change in flutter speed due to a change in the frequencies of vibration. The frequencies were adjusted by $\pm 10\%$ and the flutter analysis was performed. There continued to be no flutter problems for these cases. We analyzed test cases where the rudder system circuit stiffness varied, and it was found that modifying the circuit stiffness, comprised of the rudder torque tube, the linkage system, and the attach hardware, had a negligible effect on the flutter speed. Furthermore, a case where the rudder linkage system fails, resulting in a rudder allowed to rotate freely, showed no flutter potential in the flight regime.

Prediction of Classical Static Divergence of the Fin

In this section, we predict the static divergence of the V131 fin using classical techniques. The divergence condition is given by

$$q_{div} = \frac{K_{\alpha}}{ec^2a}, \quad (1)$$

where q_{div} is the divergence dynamic pressure, K_{α} is the stiffness per unit span of the fin that resists torsion, ec is the distance from the aerodynamic center to the elastic axis of the fin, c is the chord of the fin, and a is the slope of the lift curve. For the present analysis, $a = 2\pi/\text{rad}$. It is assumed that the elastic axis lies at the midchord and that the aerodynamic center lies at the quarterchord line, such that $e = .25$. To compute K_{α} , we recall that

$$K_{\alpha} = \omega_{\alpha}^2 I_0, \quad (2)$$

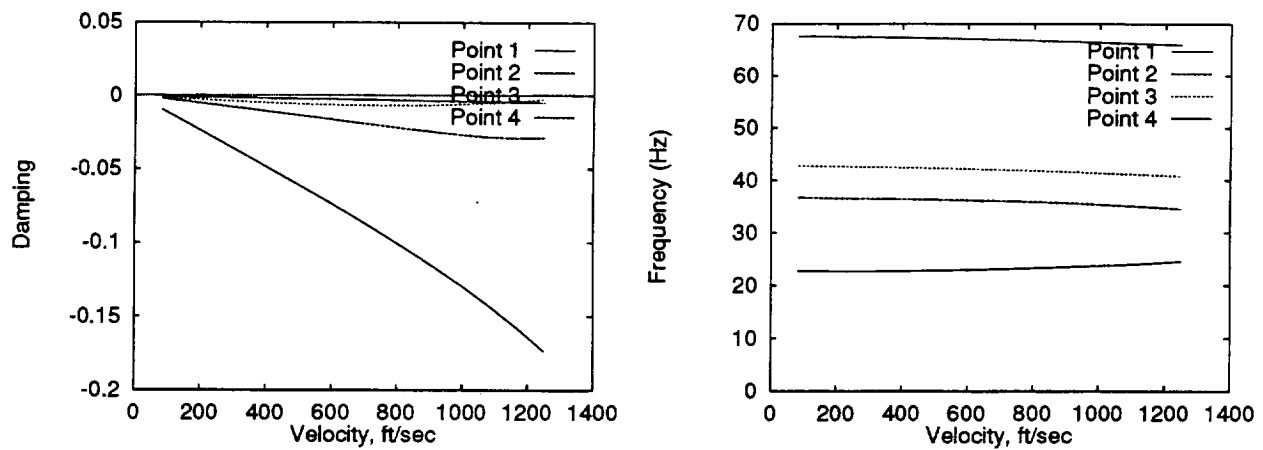


Figure 35. Damping and frequency curves for 10,000 ft.

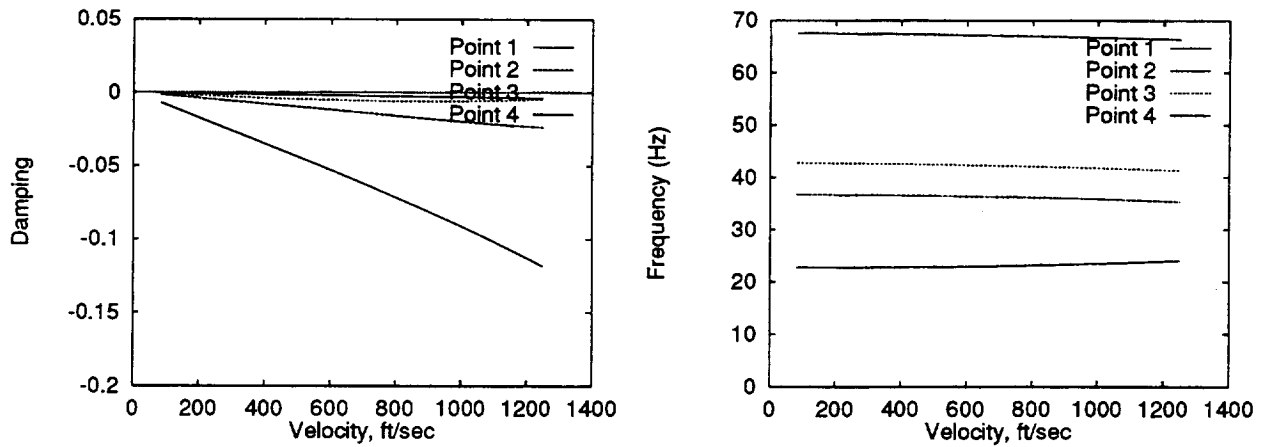


Figure 36. Damping and frequency curves for 20,000 ft.

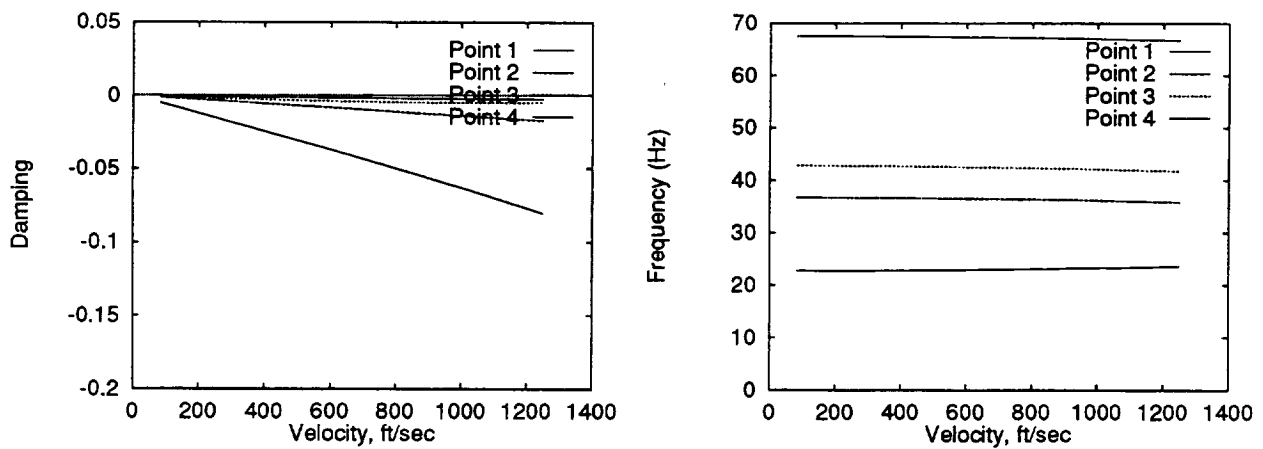


Figure 37. Damping and frequency curves for 30,000 ft.

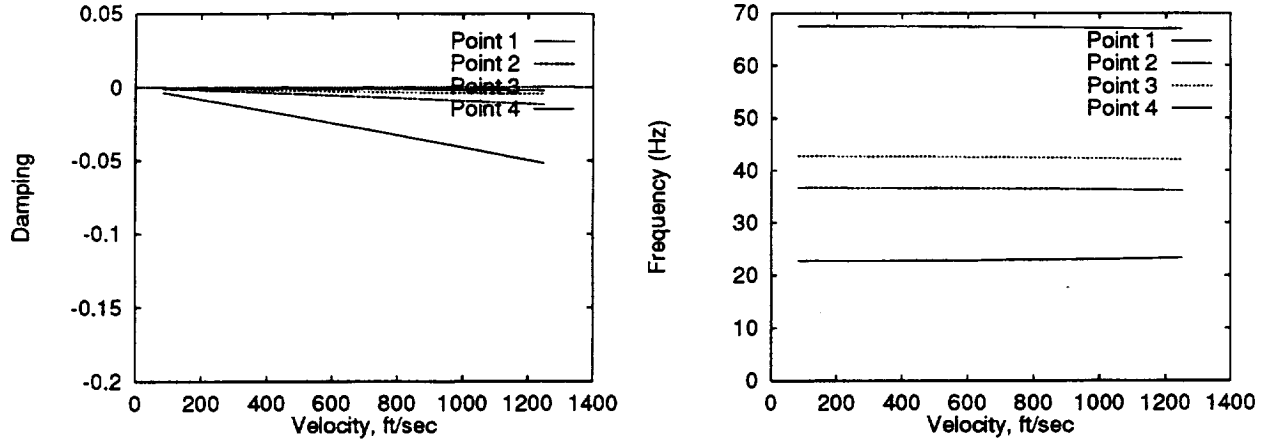


Figure 38. Damping and frequency curves for 40,000 ft.

where ω_α is the frequency of the fin in torsion, and I_0 is the mass moment of inertia per unit span of the fin, given by

$$I_0 \approx \frac{1}{12} m_t c^2. \quad (3)$$

In (3), m_t is the mass of the fin per unit span, which for the present fin is

$$m_t \approx .50517 \frac{\text{lb-sec}^2}{\text{ft}^2}. \quad (4)$$

From the modal test of the vehicle, a torsion mode with the rudder not fixed to the fin was found at 67.19 Hz, as shown in Figure 19 and at 65.34 Hz for the shimmed configuration, as shown in Figure 27. Using the lower of the two frequencies, then $\omega_\alpha = 410.54$ rad/sec. Next, using the reference chord value of $c = 62.86$ inches, then

$$K = 261916 \text{ lb/rad}. \quad (5)$$

Thus, equation (1) yields a divergence pressure of

$$q_{div} = 42.2 \text{ psi} = 6076 \text{ psf}, \quad (6)$$

which is well above the flight profile of $q = 500$ psf for the vehicle.

Aileron Buzz Prediction of the Fin

The flight regime of the V131 presents a potential transonic environment over the vehicle fins. Therefore, aileron buzz can manifest itself. NASA SP-8003 [4] recommends wind-tunnel tests in the transonic regime when

$$\frac{b\omega}{V} < 0.3, \quad (7)$$

where b is the control surface semichord in feet, ω is the control surface frequency in radians per second, and V is the free-stream velocity in feet per second. The semichord of the rudder is taken as half the distance from the rudder hinge line to the aft edge of the rudder, giving $b = 1.125$ ft. Using the test frequency associated with the free rudder configuration ($f = 36.771$ Hz) shown in Figure 14, then

$$V < \frac{(1.125)(36.771)(2\pi)}{.3} \text{ ft/sec} = 866.4 \text{ ft/sec}. \quad (8)$$

Table 2. Aileron Buzz Dynamic Pressure and Mach Number

Altitude (kft)	q_{buzz} (psf)	M_{buzz}
0	892	.77
10	658	.79
20	476	.82
30	334	.86
40	219	.88

Table 2 shows the flight altitude and the dynamic pressure and Mach number corresponding to (8). For altitudes of 20,000 ft and above, the maximum allowable flight dynamic pressure of $q = 500$ psf is greater than q_{buzz} . Additionally, the B-52 flight envelope allows for Mach 0.8 at 35,000 ft and above, which is below M_{buzz} , so buzz is not predicted while on the B-52 vehicle.

References

- [1] Bisplinghoff, R.L., and H. Ashley, *Principles of Aeroelasticity*, Dover, New York, 1962.
- [2] Fung, Y.C., *An Introduction to the Theory of Aeroelasticity*, John Wiley & Sons, New York, 1955.
- [3] *Military Specification - Airplane Strength and Rigidity Vibration, Flutter, and Divergence*, MIL-A-8870C, 1993.
- [4] *NASA Space Vehicle Design Criteria - Flutter, Buzz, and Divergence*, (3:B:1:1), NASA SP-8003, 1970.
- [5] Scanlan, R.H., and R. Rosenbaum, *Introduction to the Study of Aircraft Vibration and Flutter*, MacMillan Co., New York, 1951.

REPORT DOCUMENTATION PAGE			Form Approved OMB No. 0704-0188	
Public reporting burden for this collection of information is estimated to average 1 hour per response, including the time for reviewing instructions, searching existing data sources, gathering and maintaining the data needed, and completing and reviewing the collection of information. Send comments regarding this burden estimate or any other aspect of this collection of information, including suggestions for reducing this burden, to Washington Headquarters Services, Directorate for Information Operations and Reports, 1215 Jefferson Davis Highway, Suite 1204, Arlington, VA 22202-4302, and to the Office of Management and Budget, Paperwork Reduction Project (0704-0188), Washington, DC 20503.				
1. AGENCY USE ONLY (Leave Blank)	2. REPORT DATE May 1997	3. REPORT TYPE AND DATES COVERED NASA Technical Paper		
4. TITLE AND SUBTITLE TP 3683, X-38 Vehicle 131 Flutter Assessment		5. FUNDING NUMBERS		
6. AUTHOR(S) James P. Smith				
7. PERFORMING ORGANIZATION NAME(S) AND ADDRESS(ES) Lyndon B. Johnson Space Center Houston, Texas 77058		8. PERFORMING ORGANIZATION REPORT NUMBERS S-826		
9. SPONSORING/MONITORING AGENCY NAME(S) AND ADDRESS(ES) National Aeronautics and Space Administration Washington, D.C. 20546-0001		10. SPONSORING/MONITORING AGENCY REPORT NUMBER TP-3683		
11. SUPPLEMENTARY NOTES				
12a. DISTRIBUTION/AVAILABILITY STATEMENT Unclassified/unlimited Available from the NASA Center for AeroSpace Information (CASI) 800 Elkridge Landing Rd Linthicum Heights, MD 21090-2934 (301) 621-0390 Subject Category: 16			12b. DISTRIBUTION CODE	
13. ABSTRACT (Maximum 200 words) Contained herein are the findings from the X-38 vehicle flutter prediction program at the NASA/Johnson Space Center. The results presented show the 131 vehicle to be flutter free in the maximum flight profile of q=500 psf.				
14. SUBJECT TERMS ailerons, flutter, flutter analysis, rudders, fins, aerodynamic forces, aircraft, aerodynamic balance, damping, divergence		15. NUMBER OF PAGES 30	16. PRICE CODE	
17. SECURITY CLASSIFICATION OF REPORT Unclassified	18. SECURITY CLASSIFICATION OF THIS PAGE Unclassified	19. SECURITY CLASSIFICATION OF ABSTRACT Unclassified	20. LIMITATION OF ABSTRACT None	